

**DESIGN, MODELING AND CHARACTERIZATION OF A  
PIEZOELECTRIC ENERGY HARVESTING DEVICE**

By

**KHALID ABD ALWAHAB SULIMAN MANSOUR**

**FINAL PROJECT REPORT**

Submitted to the Department of Electrical & Electronic Engineering  
in Partial Fulfillment of the Requirements  
for the Degree  
Bachelor of Engineering (Hons)  
(Electrical & Electronic Engineering)

Universiti Teknologi PETRONAS  
Bandar Seri Iskandar  
31750 Tronoh  
Perak Darul Ridzuan

© Copyright 2013

by

Khalid Abd Alwahab Suliman Mansour, 2013

# **CERTIFICATION OF APPROVAL**

## **DESIGN, MODELING AND CHARACTERIZATION OF A PIEZOELECTRIC ENERGY HARVESTING DEVICE**

by

Khalid Abd Alwahab Suliman Mansour

A project dissertation submitted to the  
Department of Electrical & Electronic Engineering  
Universiti Teknologi PETRONAS  
in partial fulfilment of the requirement for the  
Bachelor of Engineering (Hons)  
(Electrical & Electronic Engineering)

Approved:

---

Assoc. Prof. Dr. John Ojur Dennis

Project Supervisor

UNIVERSITI TEKNOLOGI PETRONAS  
TRONOH, PERAK

May 2013

## **CERTIFICATION OF ORIGINALITY**

This is to certify that I am responsible for the work submitted in this project, that the original work is my own except as specified in the references and acknowledgements, and that the original work contained herein have not been undertaken or done by unspecified sources or persons.

---

Khalid Abd Alwahab Suliman Mansour

## ABSTRACT

The mechanical vibratory energy has been extracted based on the car engine's frequency and converted into an electrical energy by making use of a bimorph piezoelectric harvesting device; this process is called energy harvesting. The output of that energy used to power-up small electronics devices such as electronic transmitters and sensors which utilize low voltage and current (1-5 Volt / 10 - 20 mA). A cantilever of Lead-Zirconate-Titanate ( $\text{PbZrO}_3\text{TiO}_2$ ) with dimensions of ( $40 \times 10 \times 0.5$  mm) has been analyzed and it's produced an output power in the range of ( $100\mu\text{W} - 0.4\text{mW}$ ) at resonance frequency of ( $\leq 0.2$  KHz) under peak acceleration of ( $\leq 10$   $\text{m/s}^2$ ). This cantilever's targeted vibration is dynamic (damped) vibration; therefore it has been subjected into continuous vibratory force. The Static Vibration is run at the first stages to check the working force and stamina of the cantilever by applying a pulse of movement and observe the response of the transient wave of the cantilever. The project aims to design and model a bimorph piezoelectric (PZT) cantilever device uses the effects of piezoelectric property to extract the mechanical vibration that is generated based on the car engine compartment's specifications and convert it to electrical energy. Successfully, a bimorph piezoelectric harvester cantilever was designed under the optimal conditions identified in this report to extract the car engine vibration produced by dynamic vibration shaker using the typical frequencies and acceleration of the car engine and produced output power nearly 0.39 mW when converts this extracted vibration to electrical energy.

## **ACKNOWLEDGEMENTS**

First and foremost I would like to express my humble gratitude to Allah S.W.T for giving me the ability to complete this project and degree in general. Honorably thanking Universiti Teknologi PETRONAS (UTP) for providing me this chance to continue my higher education in such a amazing university. Great thanks are kept to all Electrical and Electronic Engineering Department Staff for their support and help. My utmost appreciation and gratitude towards my Final Year Project supervisor Assoc. Prof. Dr. John Ojur Dennis who provided me clear guidance and huge support, and also my Co-supervisor from Electrical and Electronics Engineering Department Senior Lecturer Dr. Mohd Haris B Mohd Khir for his support and guiding during my first stages of this project. Many thanks also go to UTP Laboratory technicians from Electrical Engineering and Mechanical Engineering Departments for their cooperation. Special thanks to Dr. Nasreen Bt Badruddin the coordinator of FYP II for supporting and advising. Not to be forgotten, all the people directly or indirectly were involved in making this project a reality, friends and colleagues. Lastly I would like to thanks all my family for their inspiring and motivation in me. All the help and sharing of information is highly appreciated in which has enabled well performance and completion of this project.

# TABLE OF CONTENTS

LIST OF TABLES .....	ix
LIST OF FIGURES .....	x
LIST OF ABBREVIATIONS .....	xi
CHAPTER 1 INTRODUCTION .....	1
1.1 Project Background .....	1
1.2 Energy Harvesting Device .....	1
1.2.1 Parameter optimization .....	2
1.2.2 Direct piezoelectric bimorph membrane cantilever.....	2
1.3 Problem Statement .....	3
1.3.1 Significant of the project .....	3
1.4 Objectives.....	3
1.5 Feasibility of the Study .....	3
CHAPTER 2 LITERATURE REVIEW .....	5
2.1 PZT Cantilever .....	5
2.2 Applications of PZT Energy Harvester .....	8
2.2.1 Energy sources for WSNs.....	8
2.2.2 Higher output power with array of PZT cantilevers.....	9
2.3 Theoretical Approach.....	10
2.3.1 Cantilever analysis.....	10
2.3.2 Cantilever mass analysis (m) .....	11
2.3.3 Proof mass .....	11
2.3.4 Cantilever frequency with a proof mass .....	12
2.3.5 Acceleration (g value).....	12
2.3.6 Expected output power .....	12
CHAPTER 3 METHODOLOGY .....	13
3.1 Project Work Flow .....	13
3.2 Project Activities .....	14
3.2.1 Mathematical modelling and calculations .....	14
3.2.2 Simulation design .....	16
3.2.3 Experimental device analysis .....	17
3.3 Tools and Equipments.....	18
CHAPTER 4 RESULTS AND DISCUSSION .....	20
4.1 Mathematical Modelling .....	20



## LIST OF TABLES

Table 1	Frequency Ranges and Acceleration of Vibration Sources .....	6
Table 2	Frequency Ranges and Acceleration of Vibration Sources .....	7
Table 3	Frequency Ranges and Acceleration of Vibration Sources .....	7
Table 4	Cantilever Design Variables .....	15
Table 5	Proof Mass Design Variables.....	15
Table 6	Expected Resonance Frequency.....	15
Table 7	Materials' Properties of Harvester Cantilever .....	16
Table 8	Hardware and Devices "Pictures are taken at the Vibration Lab Block 18- UTP" .....	18
Table 9	Calculated Results of the Cantilever and Proof Mass.....	21
Table 10	Calculated Frequency of a Cantilever with and without Proof Mass .....	21
Table 11	Generated Output Power Related to Applied Acceleration .....	30
Table 12	Comprehensive Comparison between Mathematical Modeling, Simulation Design and Experimental Analysis .....	31

## LIST OF FIGURES

Figure 1	PZT Cantilever Energy Harvester .....	5
Figure 2	The Ionization and Schematic Piezoelectric Charge Distributions (Open Circuit) .....	6
Figure 3	Main Elements of a Wireless Sensor Network (WSN) [15].....	9
Figure 4	A schematic Illustration of Piezoelectric Array Harvesting System .....	9
Figure 5	Dimensional Schematics of PZT design.....	10
Figure 6	Dynamic Damped Vibration Matched at the Maximum Power .....	10
Figure 7	Project Work Flow.....	13
Figure 8	Dimensional Schematic of PZT Cantilever with a Proof Mass.....	14
Figure 9	Bimorph PZT Cantilever in Three layers (PZT <sub>1</sub> -Cu-PZT <sub>2</sub> ) .....	14
Figure 10	CoventorWare Starting Window-UTP Block 23.....	16
Figure 11	The Three Basic Modules of CoventorWare.....	16
Figure 12	Three layers of the Cantilever Attaching Proof Mass .....	17
Figure 13	Actual Length and Width of the PZT Cantilever .....	18
Figure 14	PZT Cantilever under the Experimental Analysis-UTP Block 18 .....	19
Figure 15	The Real Dimensions of the Designed Cantilever.....	20
Figure 16	Basic Cantilever Specification in Designer Module.....	22
Figure 17	The Specifications of the Three Main Cantilever Layers.....	22
Figure 18	2-Dimensions Sketching for Cantilever, Substrate and Membrane.....	23
Figure 19	Simulation of the Cantilever Fixed on Etched Substrate and 3-D Magnified View of its Layers .....	24
Figure 20	3-D View of Meshed Cantilever Magnified in Manhattan Bricks with Element Size of 40 μm.....	25
Figure 21	Analyzed Cantilever Beam at applied Dynamic Pressure Force .....	26
Figure 22	Frequency and Generalized Acceleration at applied Pressure Force.....	26
Figure 23	The Transient Wave of the Cantilever's due to Single Pulse .....	27
Figure 24	The Transient Wave of the Cantilever Filtered by FIR Filter .....	27
Figure 25	Maximum Output Voltage at Acceleration $a = 6 \text{ m/s}^2$ .....	28
Figure 26	Maximum Output Voltage at Acceleration $a = 7 \text{ m/s}^2$ .....	29
Figure 27	Maximum Output Voltage at Acceleration $a = 10 \text{ m/s}^2$ .....	30

## LIST OF ABBREVIATIONS

AC	=	Alternating Current, Air Conditioner.
Cu	=	Copper.
CMOS	=	Complementary Metal–Oxide–Semiconductor.
CD	=	Compact Desk.
DC	=	Direct Current.
FIR	=	Finite Impulse Response.
MEMS	=	MicroElectroMechanical Systems.
PZT	=	Piezoelectric, Piezoelectricity.
RTC	=	Real Time Clock.
Si	=	Silicon.
UTP	=	Universiti Teknologi PETRONAS.
WSN	=	Wireless Sensor Network.

# CHAPTER 1

## INTRODUCTION

### 1.1 Project Background

It is well recognized that many types of motions in our daily life involve different types of mechanical vibration, for example, the movement of cars, motion of machines in manufacturers, small ovens vibration, the outer covering box of air conditioners as well as our personal computers while a CD running on it. These vibrations provide different ranges of frequencies, for instance the car engine compartment generates around 200 Hz, and small microwave oven able to produce 121 Hz and the windows next to a busy road induces up to 100 Hz [1].

The source of vibration that will be investigated in this project is the car engine vibration; it expected to generate a peak frequency of 100 to 200 Hz during normal driving. The reason that why we chose this source, because we keep using cars permanently and it has ability to produce high vibration motion, hence, with emergence of MEMS technology, this vibration can be harvested and converted into useful electrical energy and thereby this source of energy easily can be prevented from being wasted in vain.

### 1.2 Energy Harvesting Device

In order to convert parasitic mechanical vibrations that available from the environment, while keeping the compactness of the MEMS device; an energy harvesting device needs to have a low resonant frequency with high acceleration magnitude. Thus here the effects of proof mass, beam shape and damping will appear on the harvesting performance to provide output power [2].

### ***1.2.1 Parameter optimization***

The energy conversion from mechanical to electrical via a PZT beam follows steps below [3, 4]:

- Input vibration: applies acceleration to the beam structure.
- Effective mass: converts input acceleration into force.
- Beam shape: bends according to the force to result in strain along the PZT layer. Mechanical damping dissipates energy during oscillation.
- Piezoelectric layer of the beam: converts mechanical strain into electrical charge, which results in electrical damping of the vibrating beam.
- Electrodes: collects generated charge and electrical damping results.

Thereby the key parameters which affect the magnitude and efficiency of the power are: amplitude and frequency of the input vibration, effective mass of the beam, stiffness and damping coefficient of the structure [5]. All these parameters will be highlighted in details in the upcoming chapters.

### ***1.2.2 Direct piezoelectric bimorph membrane cantilever.***

The terms “Piezoelectric” or “Piezoelectricity” have been stemmed from the Greek word ‘Piezo’ which means pressure or press and the word ‘electric’ referring to electricity [6]. So the concept is referring to harvesting energy that stored in the mechanical vibration and turning it to electrical energy. The special device that will undergo to extract this energy and convert it called Piezoelectric Cantilever.

A cantilever basically is an extended beam, consists of one layer (Unimorph) or different multi-layers (Bimorph) of the suitable harvesting material. In this project we are going to use a Bimorph three layers cantilever; two layers of PZT (PZT<sub>1</sub> & PZT<sub>2</sub>) interspersed by a metal of copper layer (Cu).

The effects of piezoelectricity where the cantilever can be applied are divided into two types:

- i. *Direct piezoelectric effect*: it arises when the mechanical vibration applied to the piezoelectric cantilever, then it directly converts this vibration to electrical power, and the amount of this power is proportionally related to the intensity of vibration. This type of effect will be considered in this project.
- ii. *Indirect piezoelectric effect*: conversely of the first case, a mechanical movement

or vibration or sometimes deformation will be generated due to applied electric charge (current) to the piezoelectric material.

### **1.3 Problem Statement**

A natural frequency value up to 200 Hz is generated on the car engine at time of running, and is being wasted in vain. And it's noticeable that only short life span batteries with limited capacity are used to energize the small electronics devices. Thereby, within efficiency of 25 – 50%; a piezoelectric bimorph cantilever will be mounted on the edge of this engine to harvest this mechanical power and convert it to electric energy and can be increased according to cantilever harvesting material.

#### ***1.3.1 Significant of the project***

The significant of this project stems from being a continuous self-generating source of electric energy by only absorbing the vibration as long as a machine is running without using any external energy source, having no any negative impacts, and its direct correlation to MEMS technology made the project more significant to be done.

### **1.4 Objectives**

- i. To model and simulate a bimorph (PZT<sub>1</sub>-Cu-PZT<sub>2</sub>) piezoelectric energy harvesting device.
- ii. To characterize the vibration produced under realistic vibration of car engine using the dynamic shaker and transfer it into electrical energy source to power up small electronics instruments.

### **1.5 Feasibility of the Study**

Very advanced simulation software are required in order to conduct the modeling and analysis. CoventorWare software used to perform the simulation part. It's available at UTP, Electrical & Electronics department in Block 23. In addition to DEWEsoft software at UTP also in block 18 to be interfaced with the Dynamic Damped Shaker to perform the experimental part based on the car engine. The project's objectives

planned to be achieved within the proposed time with availability of MEMS facilities which fully prepared for the study.

## CHAPTER 2

### LITERATURE REVIEW

#### 2.1 PZT Cantilever

Vibration-based energy harvesting has received a great attention in the past decade. Research motivation in this field is due to the reduced power requirement of small electronic components, such as the wireless sensors, and to power such small electronic devices using the vibration energy available in their ambient so the requirement of an external power source or periodic battery replacement can be removed or at least minimized [7]. One end (end A) of a cantilever is fixed to the vibration source and the vibration itself going to be reflected in the other end (end B), in other word, when a beam start to vibrate the deflection will vary as a sinusoidal wave with time, this motion need to be stabilized by attaching specific size of mass called the *proof mass* to (end. B), and then the ionization through the PZT material a charge of energy will be induced at (end. B), as shown in figure 1.

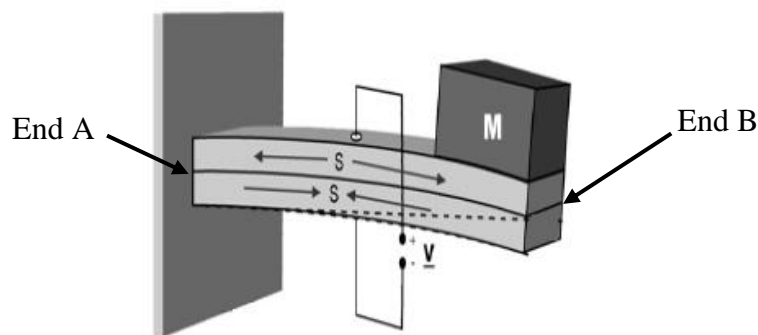


**Figure 1** PZT Cantilever Energy Harvester [8]

The ionization process occurs when the piezoelectric crystals rearrange themselves because when the vibration happens, the distance between the negative and positive charges will be changed within the crystal; hence as a result, a net polarization

appears at the surface of the piezoelectric cantilever as an open circuit measurable voltages, as it shown in figure 2.

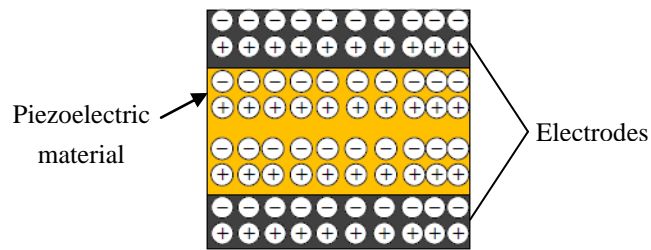


**Figure 2** The Ionization and Schematic Piezoelectric Charge Distributions (Open Circuit) [9]

A study conducted by (Nechibvute et al., 2012) [1] aims to study vibration's characteristics is certain vibration sources, and the result shown in Table 1.

**Table 1** Frequency Ranges and Acceleration of Vibration Sources [10]

Vibration sources	Peak acceleration ( $m/s^2$ )	Frequency of peak (Hz)
Car engine compartment	10-12	200
Small microwave oven	2.5	121
HVAC vents in office building	0.2-1.5	60
Windows next to a busy road	0.7	100
Notebook computer while CD is being read	0.6	75
Second story floor of busy office	0.2	100
Clothes dryer	3.5	121
Washing machine	0.5	109
Refrigerator	0.1	240

Referring to (M. Marzencki, Y. Ammar, S. Basrou, 2008) [11], they argued that the main two properties that characterized lead zirconate titanate (PZT) to be one of the important materials in PZT fabrication are: Large piezoelectric coefficient and Dielectric constant with the ability to produce more power for a given acceleration. Table 2 summarizes the output power and resonant frequencies of the mostly used materials to build up energy harvester devices.

**Table 2** Frequency Ranges and Acceleration of Vibration Sources [10]

Material	Resonant Frequency (Hz)	Power Output Range	Ref
Quartz	45 - 234	1.01 $\mu$ W	[6]
Aluminum Nitride (AlN)	200 - 1200	65 $\mu$ W	[12]
Lead Zirconate Titanate (PZT)	100 - 700	1 - 100 $\mu$ W	[13]
Barium Titanate (BaTiO <sub>3</sub> )	100 - 800	4 $\mu$ W	[7]

A study done by (M. Marzencki, Y. Ammar, S. Basrour, 2008) [11] revealed that majority of piezoelectric generators that have been fabricated use some variation of lead zirconate titanate (PZT), and the another less common material is aluminum nitride (AlN), although it has a smaller piezoelectric coefficient and dielectric constant, but it's compatible with the standard CMOS processes in fabrication of integrated circuits, because of these advantages, the project will focus on the use of PZT as the material of choice. Another discussion carried out by (J. Hyun, 2010) [14] illustrated certain considered prototype of MEMS energy harvesters, the comparison was based on the cantilever structure and attached proof mass and the results shown in Table 3.

**Table 3** Frequency Ranges and Acceleration of Vibration Sources [10]

Device Cantilever / mass	Conditions (ms <sup>-2</sup> / Hz)	Power ( $\mu$ W)	Power Density ( $\mu$ W/cm <sup>3</sup> )	Ref.
AlN / Si	4.9 / 204	0.038	10	[15]
AlN / Si	39.2 / 1368	1.97	3569	[11]
PZT / (Su-8)	106 / 13.9 K	1	37,037	[16]
PZT / Ni	9.8 / 608	2.2	10,843	[17]
PZT / Si	9.8 / 255.9	2.765	6513	[18]
AlN / Si	19.6 / 572	60	~5214	[19]
PZT / Si	19.6 / 465	2.15	3,272	[20]

However, challenges will be faced during the characterization and practical work such as the possibility of electrical losses besides choosing the appropriate resistors to measure the output current by following the accurate milli-scaling in measurements.

## **2.2 Applications of PZT Energy Harvester**

Based on the type of the external physical source has been applied (light, vibration, thermal or radio frequency) and the targeted PZT effect (direct or indirect); Piezoelectric Materials can fit into many micro sensors and actuators, such as inertia sensors, pressure sensors, tactile sensors, and flow sensors [21]. The role of PZT energy harvesters appears as the power source of these sensors, instead of using rechargeable batteries, especially when these sensors applied in harsh environment such as desert or forest to collect some data where the power source is unavailable.

In the industry field, piezoelectric cantilevers based-vibration have been used widely to extract the vibration from big machines and convert it into electrical power.

*Direct Piezoelectric effect:* accelerometers, igniters, generators, vibratory sensors, level measurements, flow measurements, medical diagnostics.

*Indirect Piezoelectric effect:* piezo-motors, laser tuning, pneumatic valves, object recognition, high resolution material testing.

### **2.2.1 Energy sources for WSNs**

The technology of Wireless Sensor Networks or (WSNs) have considered numerous studies in energy harvesting, in essence these devices have been designed to perform sensing, data collection besides monitoring certain operations [21-23]. This technology nowadays gained high much attention especially in industrial and automation fields. For instance, the electronic sensors and transmitters that used in oil and gas fields to monitor and collect the temperature, pressure, flow and level of the product. WSN consists of microcontroller unit works under low power, Micro-Electro-Mechanical (MEMS) based-sensor and transceiver works with radio frequency. In order for these sensors to work properly, it traditionally powered by batteries [24], but these batteries have limited life span, and actually one of the main factors that bounded the performance and life span of WSNs is the limited capacity of batteries [25]. Figure 3 shows clear elements of WSN.

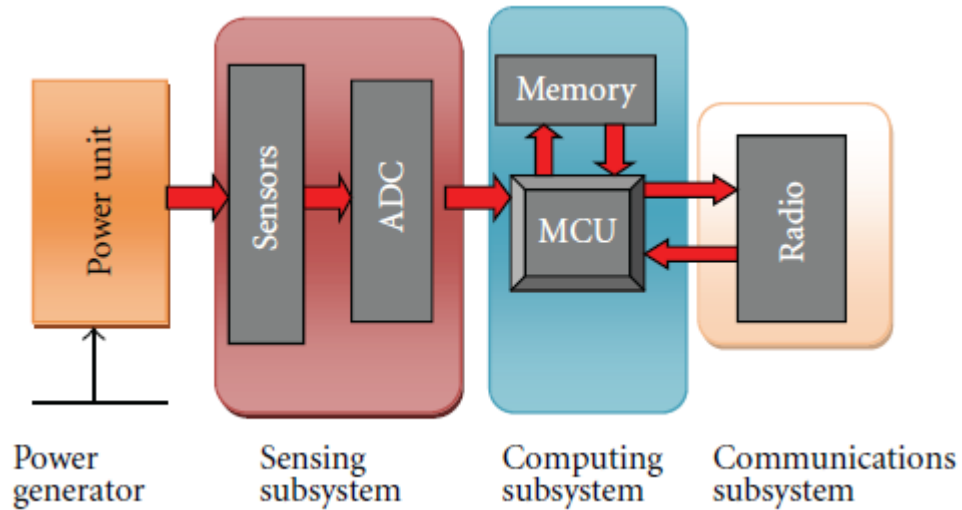


**Figure 3** Main Elements of a Wireless Sensor Network (WSN) [26]

To overcome these drawbacks; energy harvesting is the best option to produce potential infinite source of energy to power wireless sensors and embedded electronics devices.

### 2.2.2 Higher output power with array of PZT cantilevers

The more piezoelectric cantilevers attached, the more amount of power can be generated, the reason that, more layers of cantilevers able to increase the bandwidth of a resonant frequency, highlighting on that, a research conducted by (Lu F, Lee H P, Lim S P, 2004) shows the amount of output power and the number of piezoelectric layers is proportional related to each other. The essence of the research described the vibration-to-electricity energy harvesting by attaching more than one cantilever at the same time (Array Energy Harvesting System), to maximize the output power [27].

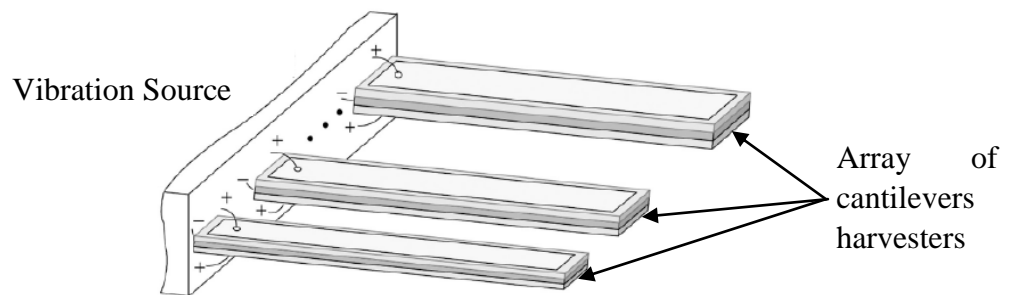


**Figure 4** A schematic Illustration of Piezoelectric Array Harvesting System [28]

## 2.3 Theoretical Approach

### 2.3.1 Cantilever analysis

To model and design the piezoelectric harvester, a bimorph 3-layers- (PZT<sub>1</sub>-Cu-PZT<sub>2</sub>) cantilever has been analyzed, and the dimensional drawing of the harvesting devices as shown in figure 5.

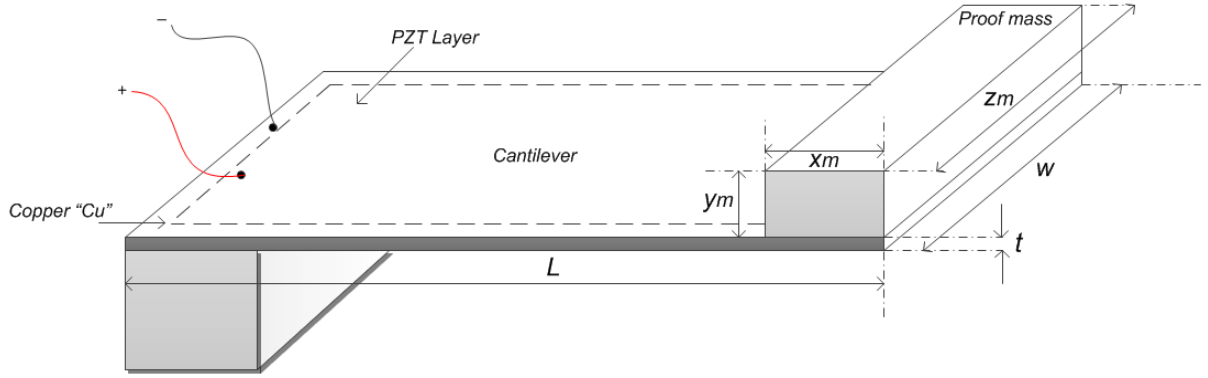


**Figure 5** Dimensional Schematics of PZT design

The maximum output power can be achieved when the resonant frequency of the cantilever matches the frequency of the vibration.

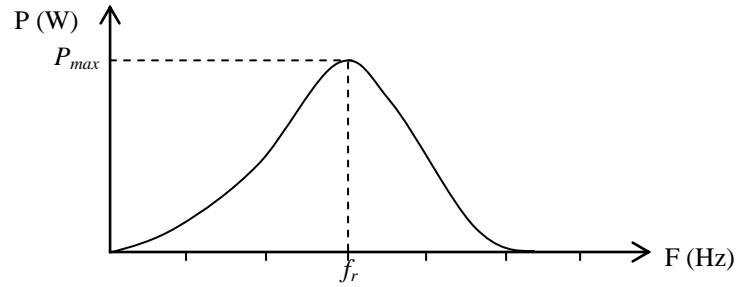


**Figure 6** Dynamic Damped Vibration Matched at the Maximum Power

The construction material for both PZT<sub>1</sub> and PZT<sub>2</sub> layer is a Lead-Zirconate-Titanate (PbZrO<sub>3</sub>TiO<sub>2</sub>). The equation that governing the Resonance Frequency ( $f_r$ ) can be found by using equation (1) below:

$$f_r = \frac{1}{2\pi} \sqrt{\frac{k}{m_{eff}}} \quad (1)$$

where  $k$  and  $m_{eff}$  are the spring constant and the effective mass of the beam respectively. The value of the spring or Stiffness constant ( $k$ ) of the cantilever can be calculated using equation (2) below:

$$k = \frac{E_{avg} \times w \times t^3}{4 \times l^3} \quad (2)$$

where  $E_{avg}$  the average of cantilever layers' young's modules and  $l$ ,  $w$ ,  $t$  are the length, width and height of the design respectively. The area of the proof mass ( $A$ ) can be obtained using equation (3):

$$A = z_m \times x_m \quad (3)$$

where  $z_m$  and  $x_m$  are the length and width of the proof mass model. However, because we are using a type of bimorph harvester cantilever, the young's modules or modules of elasticity ( $E_{avg}$ ) must be determined for all cantilever's layers, by applying equation (4):

$$E_{avg} = \sum_{i=1}^3 \frac{(E_i \times t_i)}{t_i} = \frac{E_{PZT1} \times t_{PZT1} + E_{PZT2} \times t_{PZT2} + E_{cu} \times t_{cu}}{t_{PZT1} + t_{PZT2} + t_{cu}} \quad (4)$$

### 2.3.2 Cantilever mass analysis ( $m$ )

The harvester beam mass ( $m$ ) before attaching the proof mass can be found by using equation (5):

$$m = \rho \times l \times t \times w = \rho \times A \times t \quad (5)$$

where  $\rho$  is the mass density of the cantilever, but for the 3-layers of the cantilever (PZT<sub>1</sub>, PZT<sub>2</sub> & Cu); the mass is calculated by considering the average value of the mass densities  $\rho_{avg}$ , thus we update equation (5) to be:

$$m = \rho_{avg} \times l \times t \times w \quad (6)$$

where the value of  $\rho_{avg}$  can be calculated by equation (7):

$$\rho_{avg} = \sum_{i=1}^3 \frac{(\rho_i \times t_i)}{t_i} = \frac{\rho_{PZT1} \times t_{PZT1} + \rho_{PZT2} \times t_{PZT2} + \rho_{cu} \times t_{cu}}{t_{PZT1} + t_{PZT2} + t_{cu}} \quad (7)$$

In order to achieve the resonant frequency in equation (1); we have to find the effective mass ( $m_{eff}$ ) of the beam according to equation (8):

$$m_{eff} = \frac{33}{140} \times m \approx 0.24m \quad (8)$$

### 2.3.3 Proof mass

The design parameters of the proof mass as will be discussed in the next chapter; the proof mass that will be applied here is the rubber, the total mass can be calculated using equation (9):

$$m_{pm} = \rho_{pm} \times z_m \times x_m \times y_m \quad (9)$$

where  $\rho_{pm}$  is proof mass (Rubber) density which around  $1.506 \text{ kg/m}^3$ , and  $y_m$  is the height of the proof mass design. Rubber has been chosen as a proof mass because it characterized of its high density value.

### 2.3.4 Cantilever frequency with a proof mass

When we attach the proof mass to the cantilever, the height will increase, and as opposite relation between the height and frequency; the resonant frequency will decrease, and then the total frequency ( $f_r$ ) can be found form equation (10) below:

$$f_r = \frac{1}{2\pi} \sqrt{\frac{k}{m_{eff} + m_{pm}}} \quad (10)$$

### 2.3.5 Acceleration (g value)

The acceleration of the examined vibration source which car vibration is going to be applied during the experimental, usually in MEMS technology the term “g value” is normally used to refer to acceleration, this value can be obtained by equation (11):

$$g \text{ value} = \frac{\text{actual acceleration}}{9.81} \quad (11)$$

### 2.3.6 Expected output power

In order to calculate the output power, we must attach an optimal load resistor ( $R$ ) to the cantilever, the value of this resistor taken to be  $10 \Omega$  (subject to change), and then the expected output power ( $p$ ) can be calculated using either equation (12) or directly by using equation (13) which stemmed from Ohm’s law:

$$Power(P) = \frac{\omega^2 \times w^2 \times t^2 \times A^2}{4(1 + w \times l \times \frac{\omega R}{t})} \times R \quad (12)$$

$$Power(P) = V \times I = \frac{V^2}{R} = I^2 \times R \quad (13)$$

where:  $\omega = 2\pi f$  rad/s,  $V$  and  $I$  are the voltage and current of the cantilever beam respectively.

## CHAPTER 3 METHODOLOGY

### 3.1 Project Work Flow

With mode of vibrations 1 Hz to 4 kHz, the simulation of a direct piezoelectric device has been reported in this project to be modeled using Bimorph PZT-layers separated with a layer of copper, the best frequency range will be taken during experiments. The methodology that is going to be followed in this project is shown in figure 7.

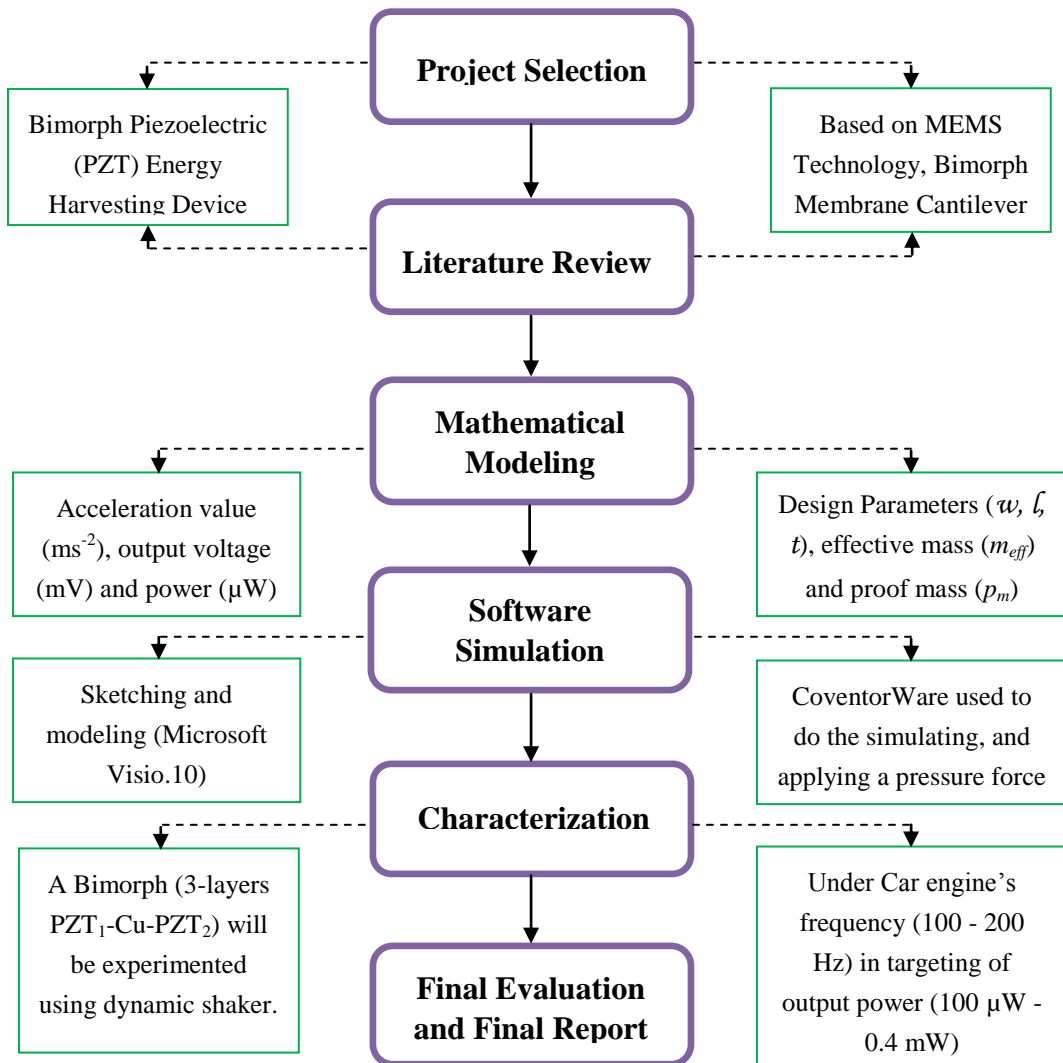


**Figure 7** Project Work Flow

### 3.2 Project Activities

The main activity of this project is to build a good design and simulation model of piezoelectric energy harvester cantilever in order to generate high electrical power from the mechanical vibratory energy under specific range of resonant frequency to power the small electronic devices such as the Real Time Clock (RTC) in the Wireless Sensors Networks (WSNs) to continually power this device as self-generating power instead of using short life span batteries with limited capacity.

#### 3.2.1 Mathematical modelling and calculations

Following the project flow, we started first by the computations part, and all the calculations have been performed by using the aforementioned equations that discussed in the literature review part with aid of Microsoft Tools.

3-D dimensional structure of the examined cantilever that has been analyzed is illustrated in figure 8, and then figure 9 shows how the cantilever attached to the Rubber proof mass to get the desired resonance frequency.

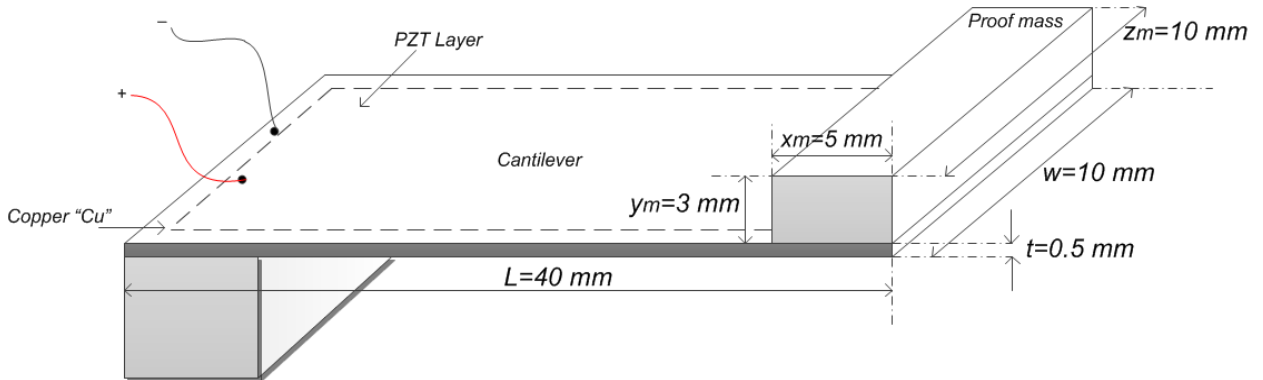


**Figure 8** Dimensional Schematic of PZT Cantilever with a Proof Mass

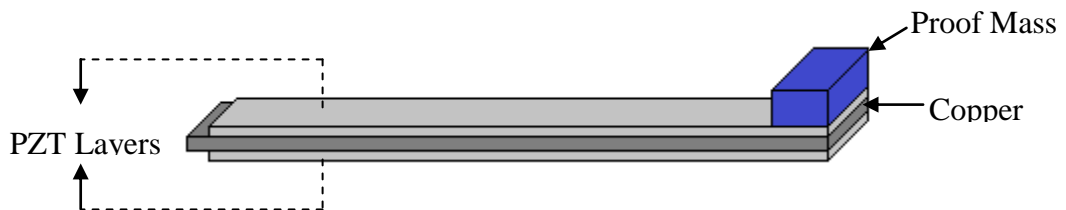


**Figure 9** Bimorph PZT Cantilever in Three layers ( $PZT_1$ -Cu- $PZT_2$ )

In order to achieve the maximum output power at the desired frequency, we need to be aware about the design variables of the cantilever in table 4 as well as the design variables of the proof mass in table 5.

**Table 4** Cantilever Design Variables

<b>Cantilever</b>		
<i>Design Parameter</i>	<i>Symbol</i>	<i>Design value</i>
Length of the Cantilever	$l$	40mm
Thickness of total cantilever layers (PZT1-Cu-PZT2)	$t$	0.5mm
Width of the cantilever	$w$	10mm
Thickness of the substrate (Copper)	$t_{cu}$	0.5mm

**Table 5** Proof Mass Design Variables

<b>Proof Mass</b>		
<i>Design Parameter</i>	<i>Symbol</i>	<i>Design value</i>
Length of the proof mass	$z_m$	10mm
Width of the proof mass	$x_m$	5mm
Thickness of the proof mass	$y_m$	3mm

Based on table 4 and table 5 above, these design criteria are subjected to change until we achieve the maximum and efficient output power. The best method that will be followed to achieve the maximum power is by modeling the proof mass dimensions. Upon applying the cantilever to car frequency, the expected resonant frequency up to ( $\leq 200\text{Hz}$ ) before attaching any proof mass, however this frequency expected to drop down nearly 126.4Hz when attaching proof mass, as in table 6.

**Table 6** Expected Resonance Frequency

Targeted cantilever's resonance frequency without proof mass	$0 \leq f_r \leq 200\text{Hz}$
Targeted Cantilever's resonance frequency including proof mass	$120 \leq f_r \leq 150\text{Hz}$

Aforementioned, the cantilever consists of 3 layers, the top layer PZT<sub>1</sub> and the bottom layer PZT<sub>2</sub>, separated by the middle layer which is Copper. Table 7 summarizes the materials properties that have been used to get the finite element analysis.

**Table 7** Materials' Properties of Harvester Cantilever

Material	Elastic Modules (E)	Mass Density ( $\rho$ )
Piezoelectric Layers (PZT1 & PZT2)	$7.2 \times 10^{10} \text{ N/m}^2$	$7.8 \text{ kg/m}^3$
Separated Metal (Copper_Cu)	$11.7 \times 10^{10} \text{ N/m}^2$	$8.9 \text{ kg/m}^3$
Proof mass (Rubber)	$0.01 \times 10^{10} \text{ N/m}^2$	$1.506 \text{ kg/m}^3$

### 3.2.2 Simulation design

Then after performing the mathematical modeling, the *Simulation Design* will be performed using CoventorWare software, the software shows and analyses the design of the cantilever beam before proceeding to the fabrication operation.



**Figure 10** CoventorWare Starting Window-UTP Block 23

CoventorWare consists of three main Modules:



**Figure 11** The Three Basic Modules of CoventorWare

During this project we'll consider the designer and analyzer modules only which meet our requirements. Then after that we'll perform the so-called Bulk Micromachining process, it used to etch deep cavities in substrate with relatively high aspect ratio. There are two types of etching process:

- i. *Front Side*: to etch the substrate or base of the cantilever from the Front side, starting at the top (just after the cantilever) going down, but it will not include the whole substrate.
- ii. *Back Side*: this etches the device from bottom to top. Back etching is the best etching for the cantilever to be very freely, so it can fluctuate very easily and smoothly, therefore back side etching will be considered in this analysis.

### 3.2.3 Experimental device analysis

The last step is the *Experimental Analysis*, where the designed model in its real dimensions with detailed layers as shown in figure 12 and figure 13, will be tested to observe the maximum output power that it can produce, and then we'll compare these outcomes with the results achieved in the calculation and simulation in next chapter.

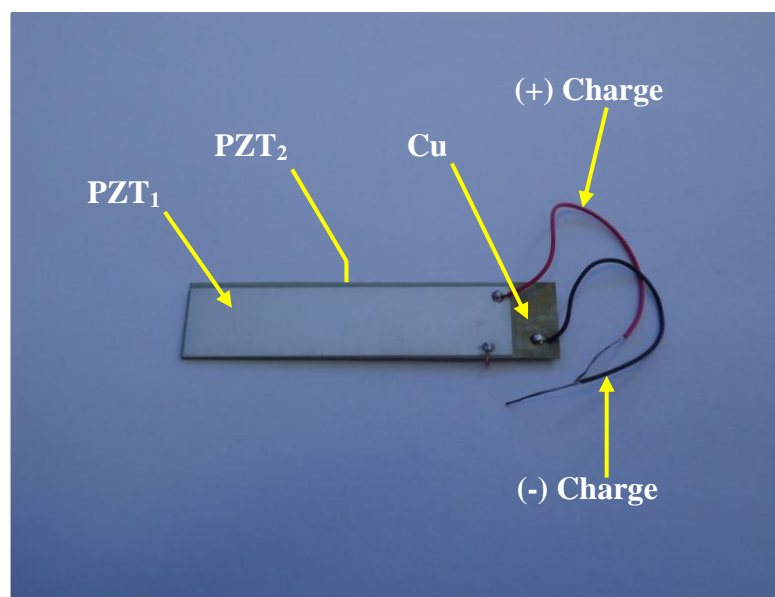


**Figure 12** Three layers of the Cantilever Attaching Proof Mass

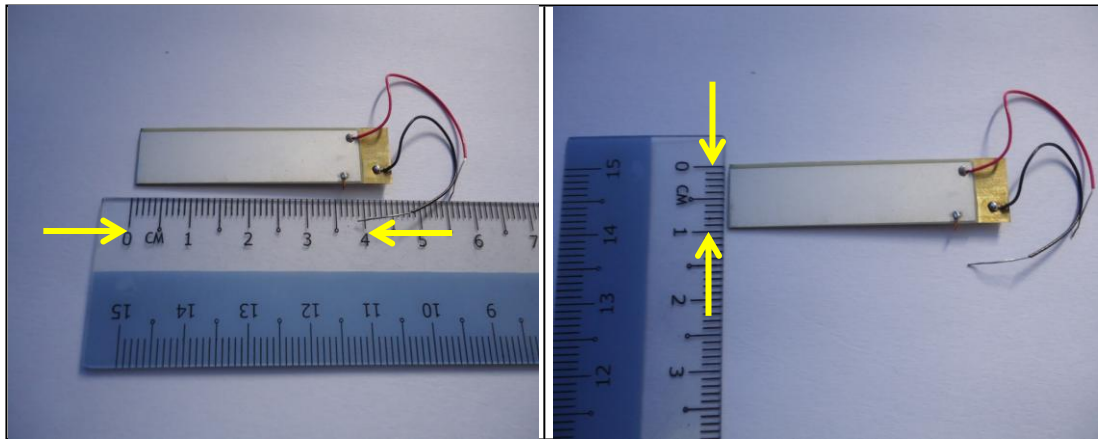


**Figure 13** Actual Length and Width of the PZT Cantilever

### 3.3 Tools and Equipments

Different electrical and devices will be used in executing required laboratory tests to examine the practical and compare it with the mathematical modeling proposal. Table 8 illustrates the group of devices that will be used to test the cantilever model.

**Table 8** Hardware and Devices “Pictures are taken at the Vibration Lab Block 18-UTP”

<b>Amplifier</b>	To increase the applied voltage to test the cantilever vibration’s response in case if indirect effect.	
<b>Shaker (IMV)</b>	To generate damped vibration within frequency range of 1 Hz - 4 kHz.	
<b>Advanced Oscilloscope</b> <i>(Dynamic Signal Analyzer)</i>	To monitor the change in frequency and output power.	
<b>Resistor Load</b>	Attaching a resistor of 10 $\Omega$ makes the current and the power measurable.	

Then when we synchronize all the devices in table 8 together, the complete experimental system will be in figure 14.

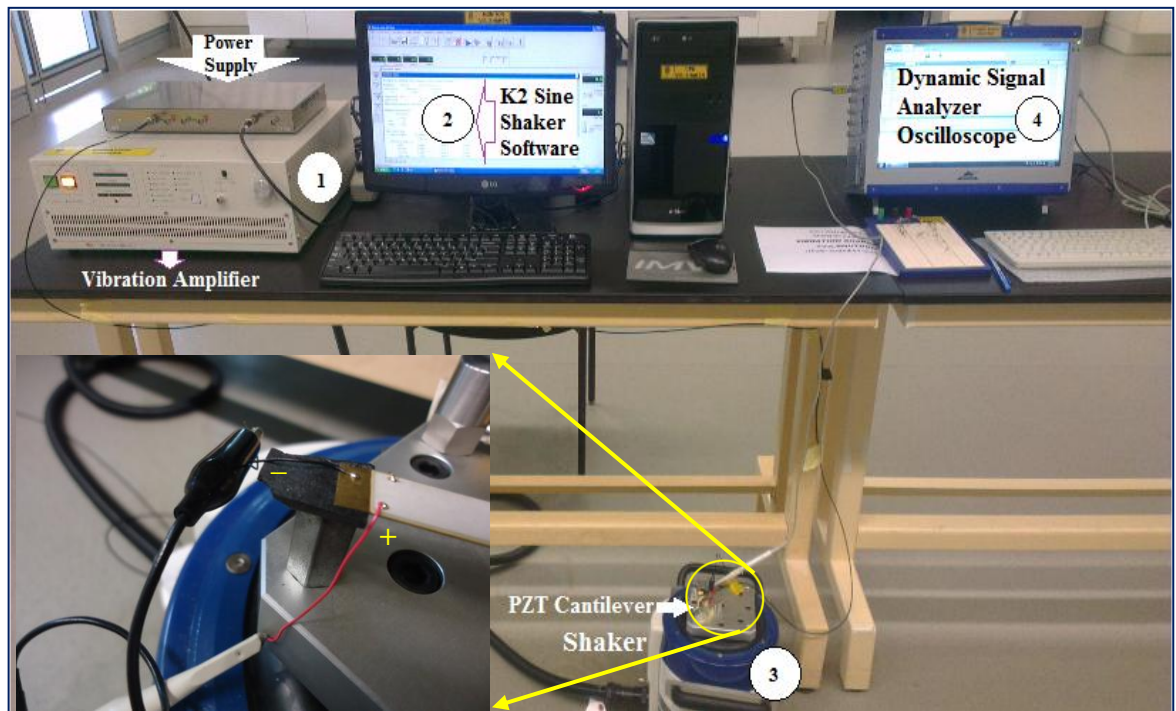


**Figure 14** PZT Cantilever under the Experimental Analysis-UTP Block 18

## CHAPTER 4

### RESULTS AND DISCUSSION

#### 4.1 Mathematical Modelling

Based on the actual dimensions of the designed cantilever, equation (7) has been used to find the average mass density of the three cantilever layers and is calculated to be  $8.02 \text{ kg/m}^3$ . And then this value used to calculate the mass of the cantilever using equation (6) and it's found to be  $1443.6 \times 10^{-6} \text{ g}$ .

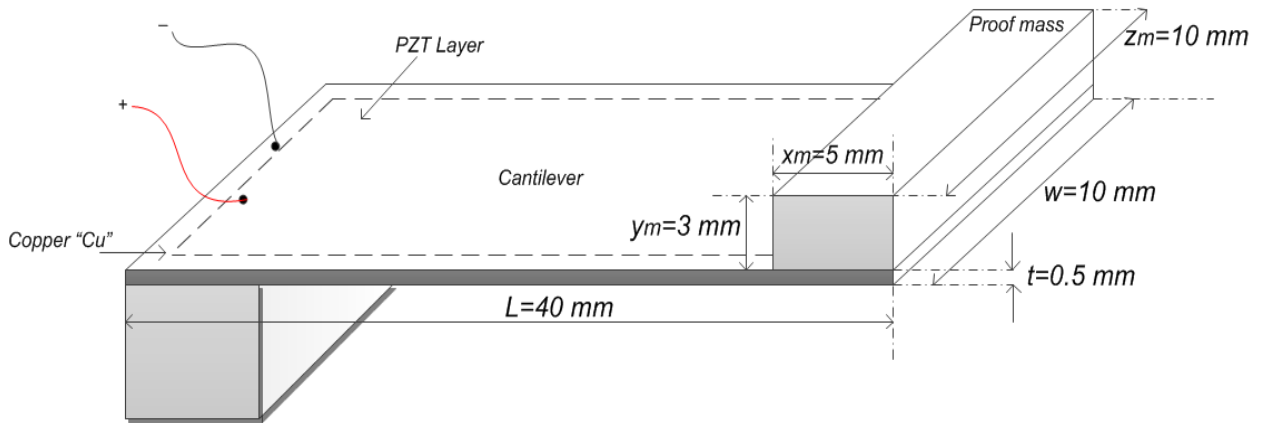


**Figure 15** The Real Dimensions of the Designed Cantilever

The effective cantilever mass is also should considered in mind, thus it can be calculated based on equation (8), and its equal  $340.28 \times 10^{-6} \text{ g}$ .

On the other hand, by considering the proof mass design -Rubber-, its total mass calculated using equation (9) and found to be  $2.89 \times 10^{-3} \text{ g}$ .

Then when we attached this proof mass to the cantilever to synchronize the fluctuation of the cantilever, the frequency will be reduced due to effective weight at end point of the cantilever. Table 9 summarizes all the calculated mathematical results of the cantilever and the proof mass.

**Table 9** Calculated Results of the Cantilever and Proof Mass

Parameter	Symbol	Result
Average Mass Density	$\rho_{avg}$	8.02 kg/m <sup>3</sup>
Mass of the cantilever	$m$	1443.6 × 10 <sup>-6</sup> g
Effective cantilever mass	$m_{eff}$	340.28 × 10 <sup>-6</sup> g
Proof mass	$m_{pm}$	2.89 × 10 <sup>-3</sup> g

The theoretical frequency that can be harvested from the car engine as a vibration source is roughly ( $\leq 200$  Hz), whereas the calculated cantilever's resonant frequency without a proof mass according to equation (1) is found to be 200.96 Hz, and then we attached the proof, the resonant frequency in this case is calculated based on equation (10), and it's equal 155.8 Hz, as illustrated in table 10. So this point concludes that the dimensions of this cantilever and proof mass are convenient to produce the targeted amount of power.

**Table 10** Calculated Frequency of a Cantilever with and without Proof Mass

Parameter	Symbol	Result
Resonant Frequency of Cantilever	$f_r$	200.96 Hz
Resonant Frequency of Cantilever and Proof Mass	$f_r$	155.8 Hz

## 4.2 Simulation Design

The simulation as aforementioned involves basically three main modules, which are architect, designer and analyzer. In this project our concentration will be on the designer and analyzer modules as main functions of the simulation.

### 4.2.1 Designer module

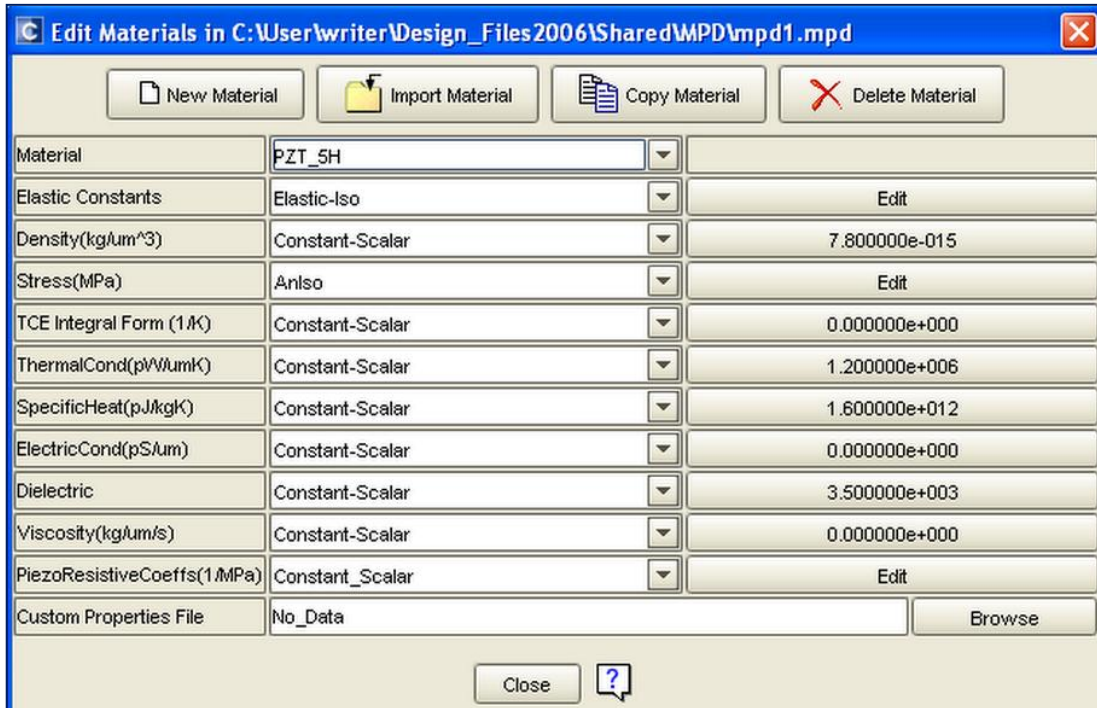


**Figure 16** Basic Cantilever Specification in Designer Module

According to figure 16, it shows cantilever material beside the basic constant values such as the young modules and the mass density, which have already discussed in the methodology. Then by considering our cantilever design and its layers compositions, figure 17 illustrates the main structural layers of the harvester. This is a very important step before we sketch the 2-Dimensional schematic, because all the upcoming steps including the analyzer module will be based on these design specification.

Number	Step Name	Action	Layer Name	Material Name	Thickness	Mask Name	Photoresist	Etch Depth	Mask Offset	Sidewall Angle	Comments
0	Substrate	Substrate	ground	SILICON_100	10000	SubstrateMask					
1	Planar Fill	Planar Fill	PZT1	PZT_5H	200						
2	Straight Cut	Straight Cut				PZT1	+		0	0	
3	Planar Fill	Planar Fill	Copper	COPPER	100						
4	Straight Cut	Straight Cut				Copper	+		0	0	
5	Planar Fill	Planar Fill	PZT2	PZT_5H	200						
6	Straight Cut	Straight Cut				PZT2	+		0	0	
7	Deep Reactive Ion Etch (DRIE)	Straight Cut				Membrane	-	10000	0	0	At higher magnification, a slight scalloping is visible.

**Figure 17** The Specifications of the Three Main Cantilever Layers

By referring to figure 17, we can see that the table sheet consists of many columns, such as the Action, Layer Name: which includes cantilever layers (PZT1, Copper, PZT2), Material Name and Thickness in micrometer scale. The column that involves the Etch Depth illustrate how deep the etching through the substrate, which is 10000  $\mu\text{m}$ . Then, we have drew our device using same CoventorWare in 2-D as a prelude for Analyzer Module later. Figure 18 describes the drawing in more details.

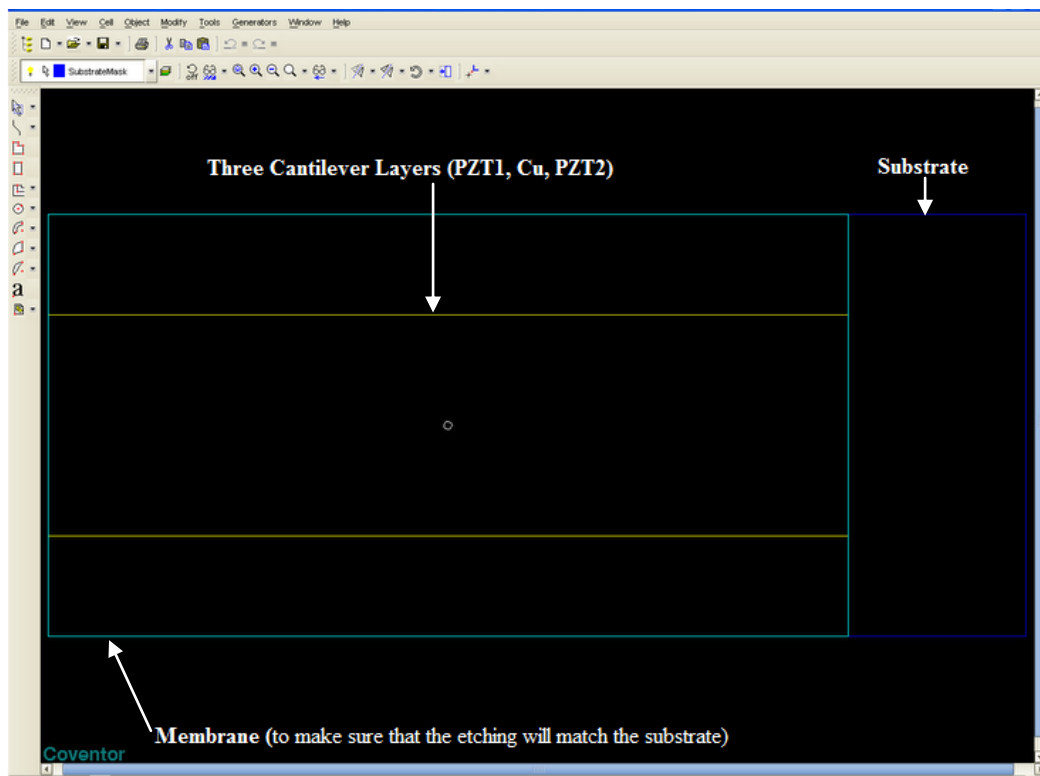


**Figure 18** 2-Dimensions Sketching for Cantilever, Substrate and Membrane

After we have designed the 2-D schematic of the design, next we must perform two important operations before we go to analyzer module:

*i. Bulk Micromachining;*

The main purpose of this deep Etching is to cut and remove out all the unnecessary parts of the examined device and highlight the cantilever layers to be only hanged in the substrate as shown in figure 19. Regarding to the magnified part in figure 19, it reveals how the thickness of the copper (in green color-100 mm) is much thinner comparing to the PZT's thicknesses (in red color-200 mm).

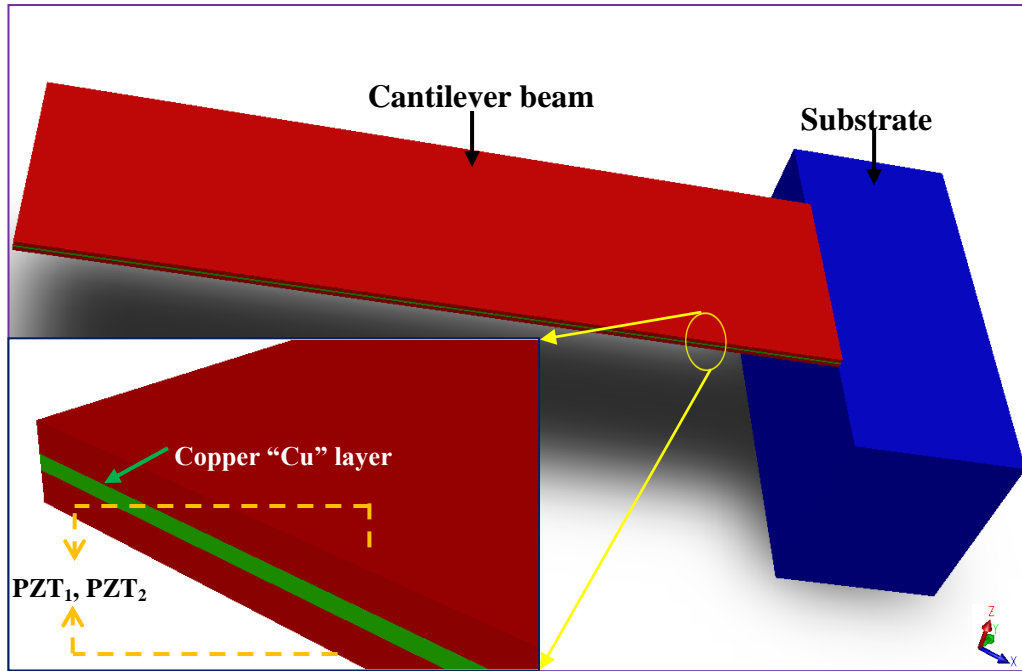


**Figure 19** Simulation of the Cantilever Fixed on Etched Substrate and 3-D Magnified View of its Layers

*ii. Meshing Process;*

This process is an essential stage before applying any pressure or vibration to the sample. An appropriate mesh greatly contributes to optimizing the accuracy and precision of calculation of the system [29]. In this case of our configuration, the physical model mesh was created using a Manhattan Bricks meshing with linear elements sized forty (40) microns in the X, Y, Z dimensions. Figure 20 shows how the cantilever appears after meshing

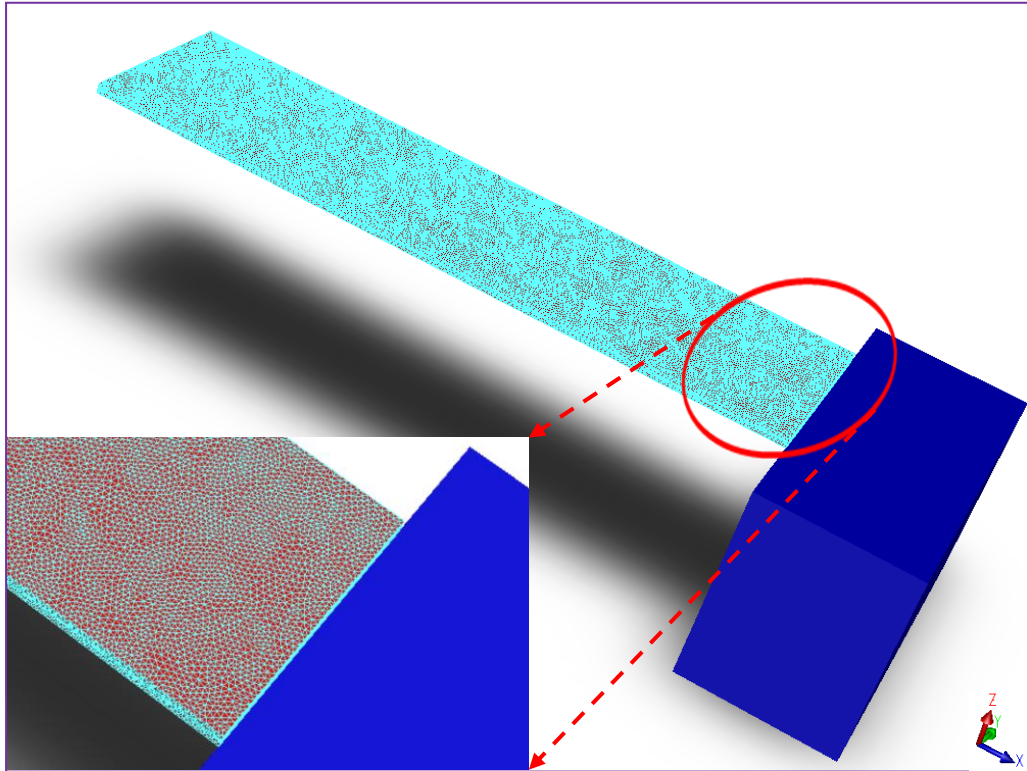


**Figure 20** 3-D View of Meshed Cantilever Magnified in Manhattan Bricks with Element Size of 40  $\mu\text{m}$

Normally in CoventorWare, meshing process comes with five types of mesh generators, each one has its own unique algorithm, which are: Mapped Bricks, Manhattan Bricks, Extruded Bricks, Surface Triangle and Tetrahedrons. The type that has been applied in this project is Manhattan Bricks as it's magnified in figure 20.

#### **4.2.2 Analyzer module**

In this module, we must verify the structure of the physical model of a designed solid model, to perform that we have applied pressure as vibration source to examine the cantilever's frequency. By applying a value of acceleration, the resonant frequency has been determined to be about 186.801 Hz as shown in figure 21, and that verify the previous frequency that we got in the mathematical modeling which were 200.96 Hz.

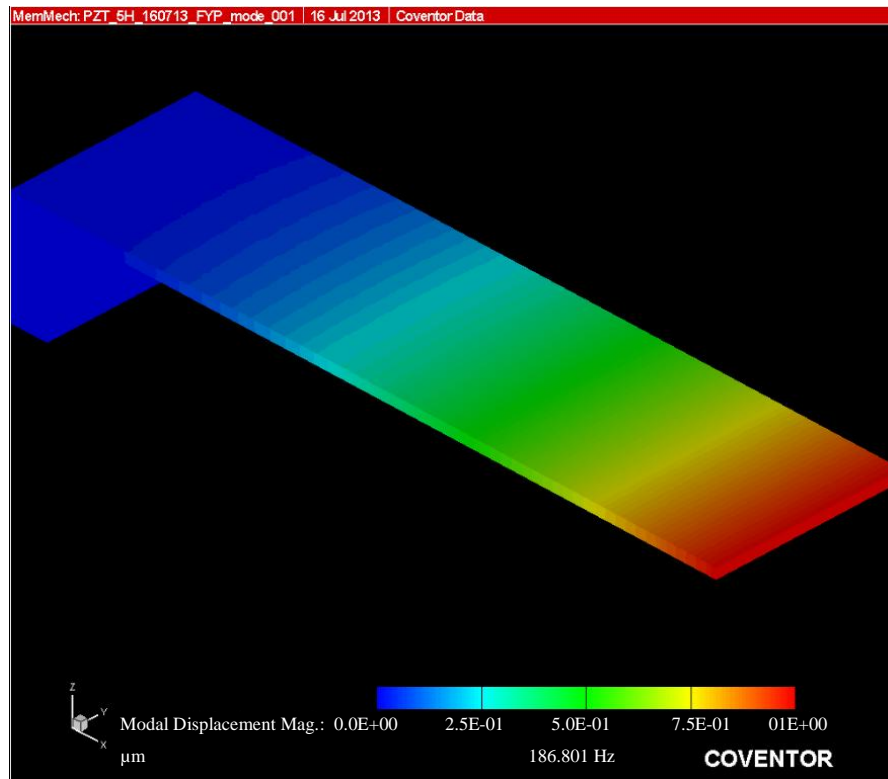


**Figure 21** Analyzed Cantilever Beam at applied Dynamic Pressure Force

After the force pressure has been applied and based on the result in figure 21, the frequency and the generated acceleration relationship is obtained from CoventorWare, and the result is shown in figure 22.

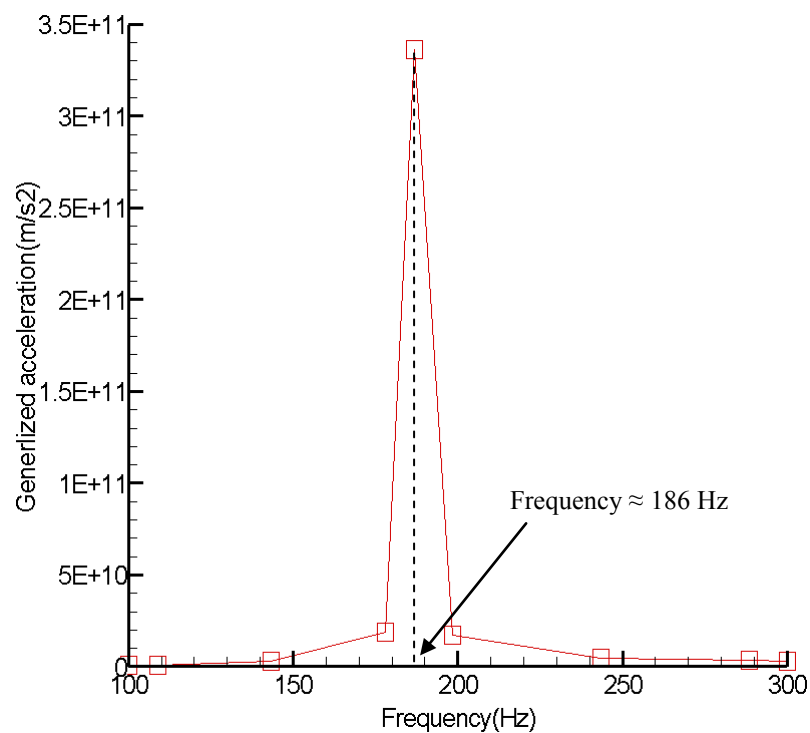


**Figure 22** Frequency and Generalized Acceleration at applied Pressure Force

### 4.3 Experimental Analysis

As has been discussed in the methodology, the experiments will be applied to the designed cantilever using different set of devices, the cantilever will be mounted based on figure 14. The initial test is to check the response of the cantilever before we start the frequency and acceleration analysis, we have applied a single pulse on the shaker to monitor the transient wave of the cantilever as show in figure 23.

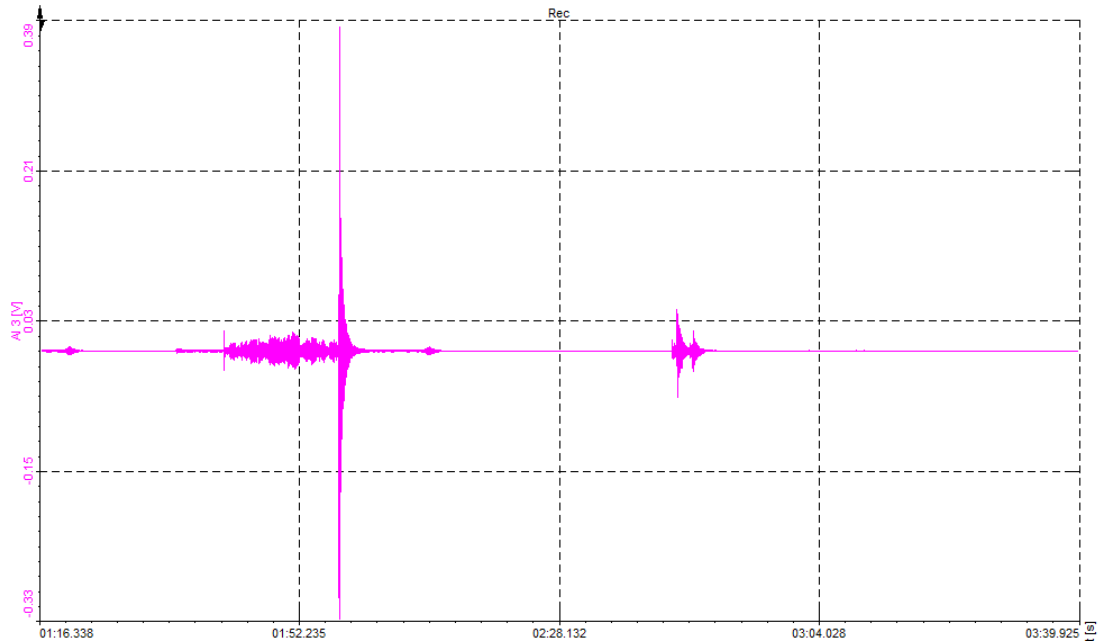


**Figure 23** The Transient Wave of the Cantilever's due to Single Pulse

The wave above contains noises while fluctuation, by applying FIR (Finite Impulse Response) filter, these noises can be eliminated, and the result shown in figure 24.

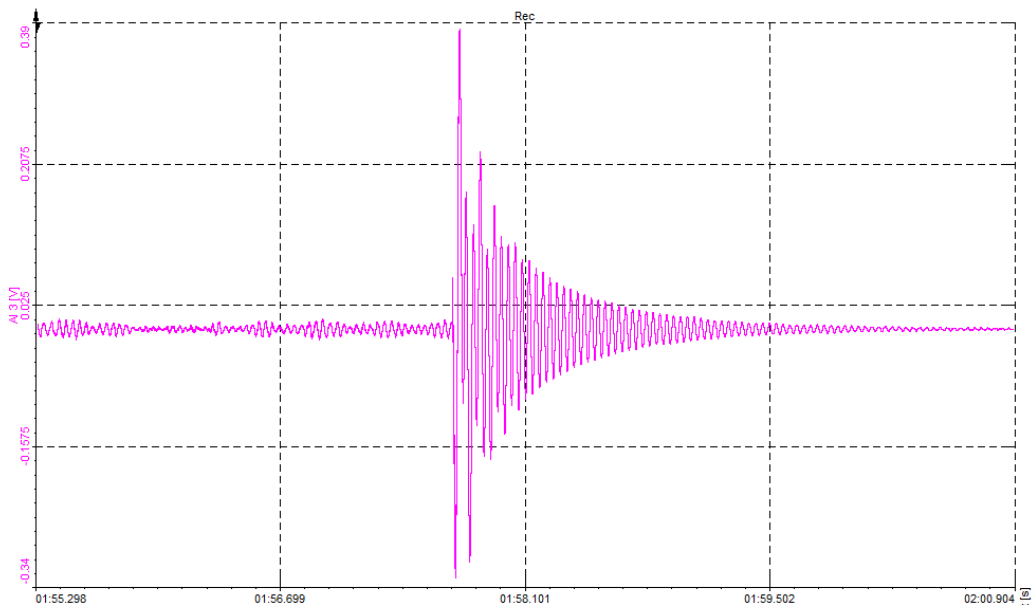


**Figure 24** The Transient Wave of the Cantilever Filtered by FIR Filter

According to Figure 23; the maximum amplitude Voltage was measured using the cursor and found to be 0.3732 V; to be sure that we applied the right type of the filter; we have checked again the maximum amplitude voltage of the filtered wave form, and cursor shows around 0.3651 V which is almost same amplitude as the original cantilever wave, so the filter didn't affect the wave form.

#### 4.3.1 Cantilever beam under frequency range 100-200 Hz

We have used the dynamic shaker to generate damped vibration same as car engine vibration in range of frequency 100 – 200 Hz and acceleration up to  $10 \text{ m/s}^2$  starting from  $6 \text{ m/s}^2$ , when the shaker start running, the fluctuation will start, and as long as we apply high accelerations values, the output voltage is expected to increase, to illustrate this relationship between acceleration and output voltage; we run the shaker by considering the cases below:

##### i. Acceleration $a = 6 \text{ m/s}^2$

By applying frequency range 100 to 200 Hz, we accelerate the shaker by  $6 \text{ m/s}^2$ , and the fluctuation wave form is shown in figure 25.

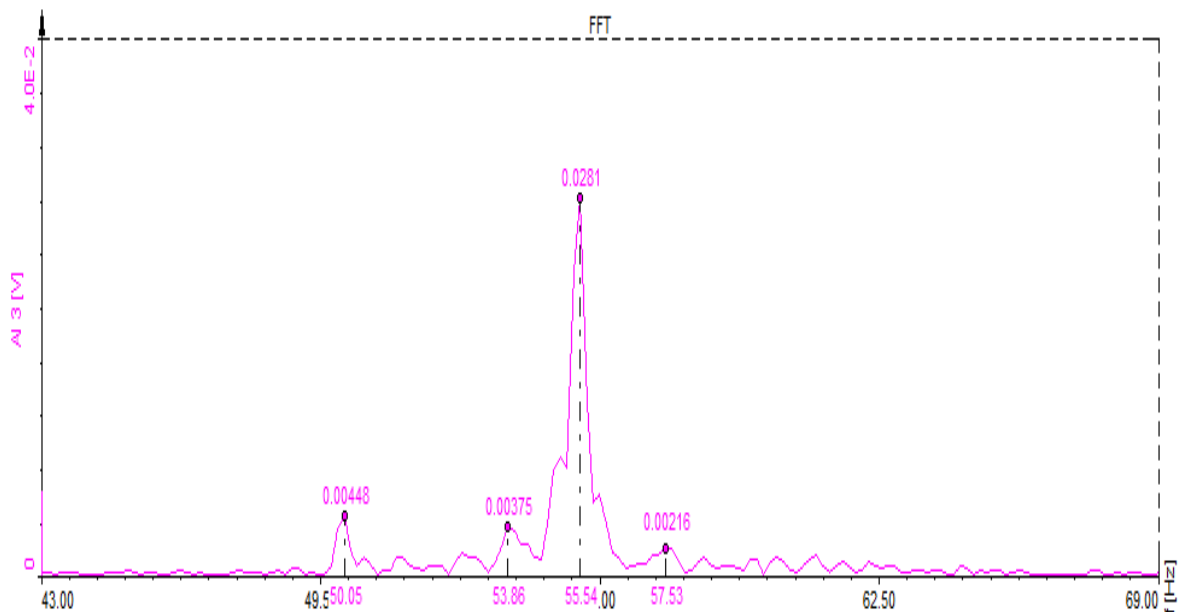


**Figure 25** Maximum Output Voltage at Acceleration  $a = 6 \text{ m/s}^2$

According to Figure 25, when the applied shaker's frequency matches the resonant frequency of the cantilever, the highest output voltage can be achieved, and as long,

and as we keep increasing the acceleration, higher voltage can be generated. From the graph, the value of output voltage around 0.0281 V at frequency 166.01 Hz, so if we consider a value of  $10 \Omega$  external resistor and according to equation (13), the output current and the produced power will be 2.81 mA and  $78.961 \mu\text{W}$  respectively.

**ii. Acceleration  $a = 7 \text{ m/s}^2$**

In this case, we are expecting higher voltage at high frequency to be generated, because of the proportional relationship between the acceleration and the voltage, thus the output voltage pulse is shown in figure 26.

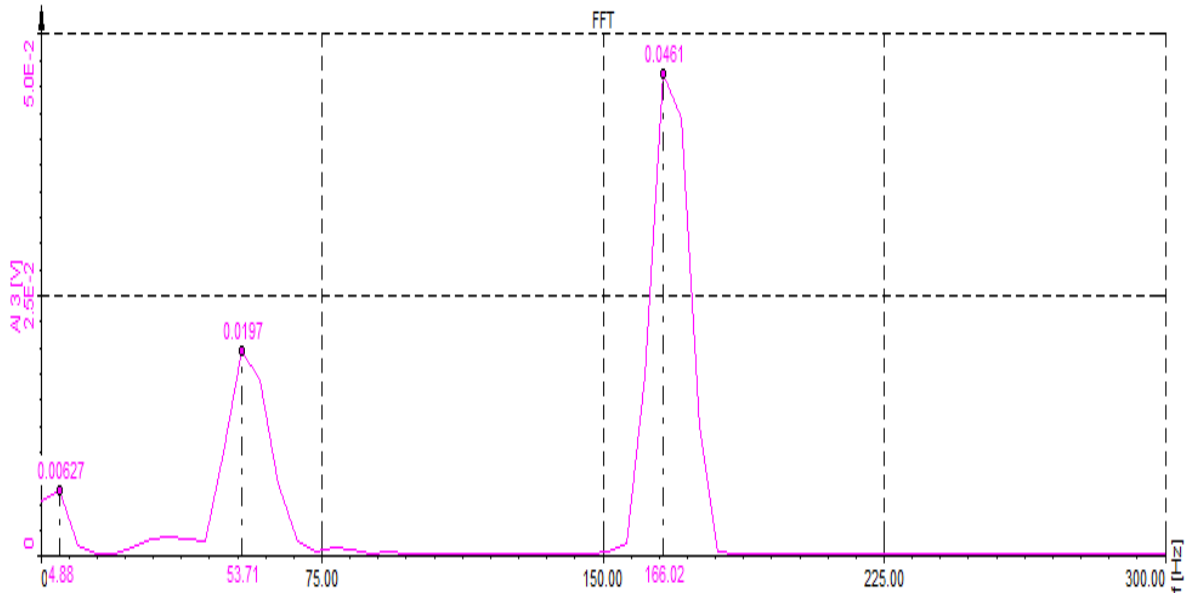


**Figure 26** Maximum Output Voltage at Acceleration  $a = 7 \text{ m/s}^2$

Comparing to the case before, the highest voltage is achieved here and around 0.0461 V, with frequency up to 166.02 Hz, which is very near to the one we got in the modeling part, so again if we attach a  $10 \Omega$  resistor to measure the current, we'll get a value of 4.61 mA, therefore the induced power around 0.213 mW which is bigger compare to case (i).

**iii. Acceleration  $a = 10 \text{ m/s}^2$**

The natural acceleration for a car engine compartment normally up to  $10 \text{ m/s}^2$ , so if we apply in this case acceleration of  $10 \text{ m/s}^2$ , for sure higher power can be introduced, to confirm that, figure 27 proofs the output voltage pulse.

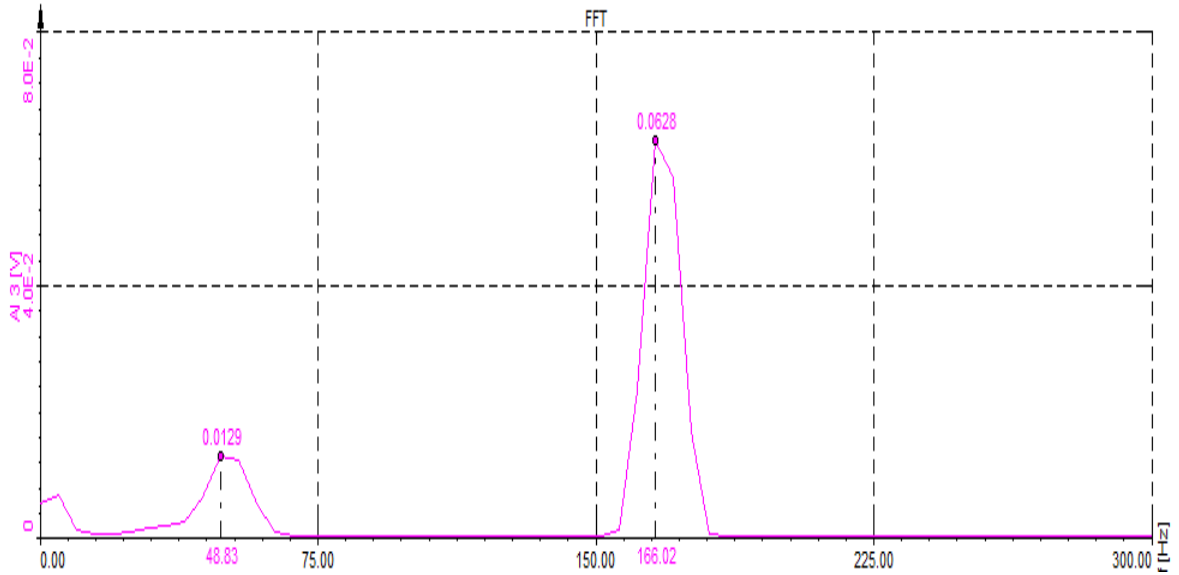


**Figure 27** Maximum Output Voltage at Acceleration  $a = 10 \text{ m/s}^2$

Now by referring to figure 26 and figure 27; we are now able to say that the resonant frequency of this cantilever is 166.02 Hz, because even though we increased the acceleration from  $7 \text{ m/s}^2$  to  $10 \text{ m/s}^2$ , we get higher voltage but the frequency of the cantilever didn't change and this also proof the result that we got on the modeling part. The output voltage in this case equal 0.0628 Volt, and with  $10 \Omega$ , the AC induced current around 6.28 mA and output power up to 0.39 mW. Table 11 summarizes the experimental results that we achieved for the three examined cases.

**Table 11** Generated Output Power Related to Applied Acceleration

Acceleration ( $\text{m/s}^2$ )	Output Voltage (V)	Output Current (mA)	Output Power (mW)	Resonant Frequency (Hz)
6	0.0281	2.81	0.0789	166.01
7	0.0461	4.61	0.213	166.02
<b>10</b>	<b>0.0628</b>	<b>6.28</b>	<b>0.39</b>	<b>166.02</b>

#### 4.4 Results Comparison

As a conclusion for this chapter, a comparison between the modeling, simulation and characterization is summarized in table 12 to illustrate the small variation that we achieved in these scenarios.

**Table 12** Comprehensive Comparison between Mathematical Modeling, Simulation Design and Experimental Analysis

<b>Mathematical Modeling</b>	<i>Average Mass Density</i> (Kg/m <sup>3</sup> )	<i>Mass of the cantilever</i> (μg)	<i>Effective cantilever mass</i> (μg)	<i>Proof mass</i> (mg)	<i>Resonant Frequency</i> (Hz)	<i>Resonant Variation</i> (%)
	8.02	1443.6	340.28	2.89	200.96	-
<b>Simulation Design</b> (CoventorWare)	<i>Etching Depth</i> (μm)		<i>Meshing Element Size</i> (μm)		<i>Resonant Frequency</i> (Hz)	<i>Resonant Variation</i> (%)
	1000		40		186.801	7.05
<b>Experimental Analysis</b>	<i>Acceleration</i> (m/s <sup>2</sup> )	<i>Output Voltage</i> (V)	<i>Output Current</i> (mA)	<i>Output Power</i> (mW)	<i>Resonant Frequency</i> (Hz)	<i>Resonant Variation</i> (%)
	10	0.0628	6.28	0.39	166.02	11.1

Even though this small variation was expected, but the reason why it's introduced; because each analysis should be performed perfectly and without considering any noise or other external factors.

## **CHAPTER 5**

### **CONCLUSION AND RECOMMENDATIONS**

#### **5.1 Conclusion**

A Bimorph PZT Cantilever has been modeled based on dual PZT-5H layers separated by a layer of Copper. The resonant frequency of this cantilever has been calculated in the modeling part and found to be 200.96 Hz. Thus, with very accurate and advanced simulation Software (CoventorWare); the simulation is performed to design the targeted device using, by applying only the Designer and Analyzer Modules, and performing a Bulk Micromachining process, the results in more details were shown in the previous chapter. Then the designed cantilever harvester had applied to typical car engine compartment specifications using vibration shaker under frequency up to 200 Hz, and acceleration in range of 6 to 10 m/s<sup>2</sup> which equal 0.61 g to 1.02 g value. Finally, the output power also has been calculated by attaching an optimal resistor of 10  $\Omega$  to the cantilever while it was running under acceleration 1.02 g, and according to the maximum output voltage achieved 0.0628 Volt the power is 0.39 mW.

The project investigates the capability of harvesting the energy from the mechanical vibration and converting it into useful electrical energy. This energy harvesting based on modeling and characterizing bimorph energy harvester cantilever of lead zirconate titanate (PbZrO<sub>3</sub>TiO<sub>2</sub>) specified as (40 mm×10 mm×0.5 mm) with expected output power to be generated (100  $\mu$ W - 0.4 mW) at resonance frequency of ( $\leq$  200 Hz) for peak acceleration of (6 - 10 m/s<sup>2</sup>). The targeted vibration is damped vibration which is the most widely used to generate the power continuously.

## **5.2 Recommendations**

Upon achieving the main objective of this project with aforementioned specifications, the recommended and suggested improvement for future work to build cantilevers by targeting lower resonant frequency with suitable proof mass to be added to take advantage of all surrounding vibrations, furthermore the challenge will exist in improving the scale down to Micro scale based on MEMS properties and performing multi-meshing CoventorWare processes for further analyze.

## REFERENCES

- [1] A. Nechibvute, A. Chawanda, P. Luhanga. (2012) Piezoelectric Energy Harvesting Devices: An Alternative Energy Source for Wireless Sensors.
- [2] G.K. Lesieutre, G.A. Ottman, and H.F. Hofmann, *Journal of Sound and Vibration*, 269, 991–1001 (2004).
- [3] H.A. Sodano, D.J. Inman, and G. Park, *The Shock and Vibration Digest*, 36, 3, PP197 (2004).
- [4] B.L. Wardle, N.E. DuToit, and S.G. Kim, *Intergrated Ferroelectric*, accepted for publication.
- [5] J.J. Bernstein, J. Bottari, K. Houston, G. Kirkos, R. Miller, B. Xu, Y. Ye, and L.E. Cross, *IEEE 1999 Ultrasonics Symposium* (Lake Tahoe, NV, Oct. 18–20 1999).
- [6] Liu C. (2010) Piezoelectric Sensing and Actuation: *Foundation of MEMS*, 2<sup>nd</sup> ed, pp269-285.
- [7] Priya S, Inman D. (2009) Piezoelectric and Electromagnetic Energy Harvesting: *Energy Harvesting Technologies*, pp 4 – 20.
- [8] S P Beeby, R N Torah, M J Tudor, P Glynne-Jones, T O'Donnell, C R Saha and S Roy, "A micro electromagnetic generator for vibration energy harvesting" *J. Micromech. Microeng.* 2007, 17, 1257–1265.
- [9] Piefort, V., *Finite Element Modelling of Piezoelectric Active Structures*. Doctoral thesis, Active Structures Laboratory, Department of Mechanical Engineering and Robotics, Universit´e Libre de Bruxelles, 2000-2001.
- [10] F. G. Carlos, H. I. Pablo, G. H. Joaquin., and A. P. Jesus, "Wireless sensor networks and applications: a survey," *International Journal of Computer Science and Network Security*, vol. 7, no. 3, 2007.
- [11] Marcin Marzencki, Yasser Ammar, Skandar Basrour, "Integrated power harvesting system including a mems generator and a power management circuit" *Sensors and Actuators A* 2008, 145-146 363-370.
- [12] D. Shen, J.H. Park, J. Ajitsara, S.Y. Choe, H.C. Wickle III, D.J. Kim, *The design, fabrication and evaluation of a MEMS PZT cantilever with an integrated Si proof mass for vibration*.
- [13] Energy harvesting, *Journal of Micromechanics and Microengineering*, 18 (2008) 055017.
- [14] J. hyun. (2010). Development of MEMS Piezoelectric Energy Harvesters, *Energy Harvesting Technologies*.

- [15] Y.B. Jeon, R. Sood, J.-h. Jeong, S.-G. Kim, “*Mems power generator with transverse mode thin film pzt*” *Sensors and Actuators A* 2005,12 216-22.
- [16] H. B Fang, J. Z. Liu, Z. Y. Xu, L. Dong, L. Wang, D. Chen, B. C. Cai, and Y. Liu, “*Fabrication and performance of mems-based piezoelectric power generator for vibration energy harvesting*” *J. Microelectronics* 2006,37 1280-1284.
- [17] B S Lee, S C Lin, W J Wu, X Y Wang, P Z Chang and C K Lee, “*Piezoelectric MEMS generators fabricated with an aerosol deposition pzt thin film*” *J. Micromech. Microeng.* 2009,19 065014.
- [18] R Elfrink, T M Kamel, M Goedbloed, S Matova, D Hohlfeld, Y van An del and R van Schaijk, “*Vibration energy harvesting with aluminum nitride-based piezoelectric devices*” *J. Micromech. Microeng.* 2009,19 094005.
- [19] Dennis. J. O, Ahmed. A. Y, Mohamad Saad. M. N, *Design, Simulation, Modeling and Characterization of Micromachined Microcantilever using CoventorWare Software*, IEEE conference publication, (2010), pp. 820 – 823.
- [20] Zimmerman WBJ. *Multiphysics Modeling With Finite Element Methods (Series on Stability, Vibration and Control of Systems, Serie)*. World Scientific Publishing Co., Inc. River Edge, NJ, USA, 2006.
- [21] S. R. Anton and H. A. Sodano, “A review of power harvesting using piezoelectric materials (2003-2006),” *Smart Materials and Structures*, vol. 16, no. 3, article R01, pp. R1–R21, 2007.
- [22] G. K. Ottman, H. F. Hofmann, A. C. Bhatt, and G. A. Lesieutre, “Adaptive piezoelectric energy harvesting circuit for wireless remote power supply,” *IEEE Transactions on Power Electronics*, vol. 17, no. 5, pp. 669–676, 2002.
- [23] S. Roundy, P. K. Wright, and J. Rabaey, “A study of low level vibrations as a power source for wireless sensor nodes,” *Computer Communications*, vol. 26, no. 11, pp. 1131–1144, 2003.
- [24] L. Chalard, D. Helal, L. Verbaere, A. Wellig, and J. Zory, “Wireless sensor networks devices: overview, issues, state-of-the-art and promising technologies,” *ST Journal of Research*, vol. 4, no. 1, pp. 4–8, 2007.
- [25] W. H. Liao, D. H. Wang, and S. L. Huang, “Wireless monitoring of cable tension of cable-stayed bridges using PVDF piezoelectric films,” *Journal of Intelligent Material Systems and Structures*, vol. 12, no. 5, pp. 331–339, 2001.
- [26] V. Raghunathan, C. Schurgers, S. Park, and M. B. Srivastava, “Energy-aware wireless microsensor networks,” *IEEE Signal Processing Magazine*, vol. 19, no. 2, pp. 40–50, 2002.
- [27] Lu F, Lee H P, Lim S P. “Modeling and analysis of micro piezoelectric power generators for micro-electromechanical-systems applications.” *Smart Mater, Struct.* 13(2004) 57-63.

[28] Xue, H.A., Y.T. Hu, and Q.M. Wang, *Broadband piezoelectric energy harvesting devices using multiple bimorphs with different operating frequencies*. IEEE Transactions on Ultrasonics Ferroelectrics and Frequency Control, 2008. **55**(9): p. 2104-2108.

[29] X. Jiang, J. Polastre, and D. Culler, "Perpetual environmentally powered sensor networks," in Proceedings of the 4th International Symposium on Information Processing in Sensor Networks (IPSN '05), pp. 463–468, April 2005.

## **APPENDICES**

**APPENDIX A**  
**PROJECT KEY MILESTONE**

No	Activities	Date	
1	<i>Submission of Proposal Defense Report</i>	<i>20 Feb. 2013</i>	(Week 6)
2	<i>Proposal Defense (Oral Presentation)</i>	<i>11 - 15Mar. 2013</i>	(Week 9)
3	<i>Submission of Interim Draft Report</i>	<i>10 April 2013</i>	(Week 13)
4	<i>Submission of Interim Final Report</i>	<i>18 April 2013</i>	(Week 14)
5	<i>Submission of Progress Report</i>	<i>10 July 2013</i>	(Week 8)
6	<i>ELECTREX (Pre-EDX)</i>	<i>31 July 2013</i>	(Week 11)
7	<i>Submission of Draft Report</i>	<i>12 August 2013</i>	(Week 13)
8	<i>Submission of Final Report</i>	<i>19 August 2013</i>	(Week 14)
9	<i>Submission of Technical Paper</i>	<i>19 August 2013</i>	(Week 14)
10	<i>Oral Presentation (VIVA)</i>	<i>26 - 28 Aug. 2013</i>	(Week 15)
11	<i>Final Report (Hard Cover)</i>	<i>17 September 2013</i>	(Week 18)

**APPENDIX B**  
**PROJECT GANTT CHART**

No	Activities	1	2	3	4	5	6	7	8	9	10	11	12	13	14	
1	<i>Topic Selection / Proposal</i>	■	■													<b>F Y P I</b>
2	<i>Preliminary Research Work</i>		■	■	■	■										
3	<i>Submission of Extended Proposal Report</i>						★									
4	<i>Proposal Defense (Oral Presentation)</i>							■	■							
5	<i>Project Work Continuation (Modeling Design)</i>									■	■	■	■	■		
6	<i>Submission of Interim Draft Report</i>													★		
7	<i>Submission of Interim Final Report</i>														★	
8	<i>Project Work (Experimental Design, Vibration lab)</i>	■	■	■	■	■										<b>F Y P II</b>
9	<i>Project Work (Simulation Design, CoventorWare)</i>						■	■								
10	<i>Submission of Progress Report</i>								★							
11	<i>Project Work Continuation</i>								■	■	■					
12	<i>ELECTREX (Pre-EDX)</i>											★				
13	<i>Project Work Continuation</i>											■	■			
14	<i>Submission of Draft Report</i>													★		
15	<i>Submission of Final Report</i>														★	
16	<i>Submission of Technical Paper</i>														★	
17	<i>Oral Presentation (VIVA)</i>	(Week 15)														
18	<i>Final Report (Hard Cover)</i>	(Week 18)														

# APPENDIX C

## DEWESOFT 7.0.3 SOFTWARE UTILIZED IN THE EXPERIMENTAL ANALYSIS

The screenshot displays the DEWESOFT 7.0.3 software interface. At the top, there are menu options: Acquisition, Analysis, Setup files, Ch. setup, and Measure. Below the menu is a toolbar with icons for Store, Save, Save as, File details, Storing, Analog, and Math. The main area shows a configuration table for 8 slots. The table includes columns for Slot, On/Off status, Channel Name, Amplifier, Physical Values, Calibration, and Setup. Slot 0 is 'Used' and has a value of -0.904 / 1.031 V. Slots 1 through 7 are 'Unused' and have various physical values ranging from -0.915 V to -2.774 V. The interface also shows a dynamic acquisition rate of 5000 Hz/ch and options for external clock and start on external trigger.

SLOT	ON/OFF	C	NAME	AMPLIFIER	PHYSICAL VALUES	CAL	SETUP
0	Used	AI 0	Daqcard direct	5V	-0.904 / 1.031 V	Zero	Set ch. 0
1	Unused	AI 1	Daqcard direct	5V	-0.915 / 1.026 V	Zero	Set ch. 1
2	Unused	AI 2	Daqcard direct	5V	-1.973 / 2.102 V	Zero	Set ch. 2
3	Unused	AI 3	Daqcard direct	5V	-0.898 / 1.036 V	Zero	Set ch. 3
4	Unused	AI 4	Daqcard direct	5V	-3.401 / 3.495 V	Zero	Set ch. 4
5	Unused	AI 5	Daqcard direct	5V	-3.495 / 3.618 V	Zero	Set ch. 5
6	Unused	AI 6	Daqcard direct	5V	-0.372 / 0.482 V	Zero	Set ch. 6
7	Unused	AI 7	Daqcard direct	5V	-2.774 / 2.899 V	Zero	Set ch. 7

**APPENDIX D**  
**VIBRATION AND VOLTAGE AMPLIFIER - UTP BLOCK 18**



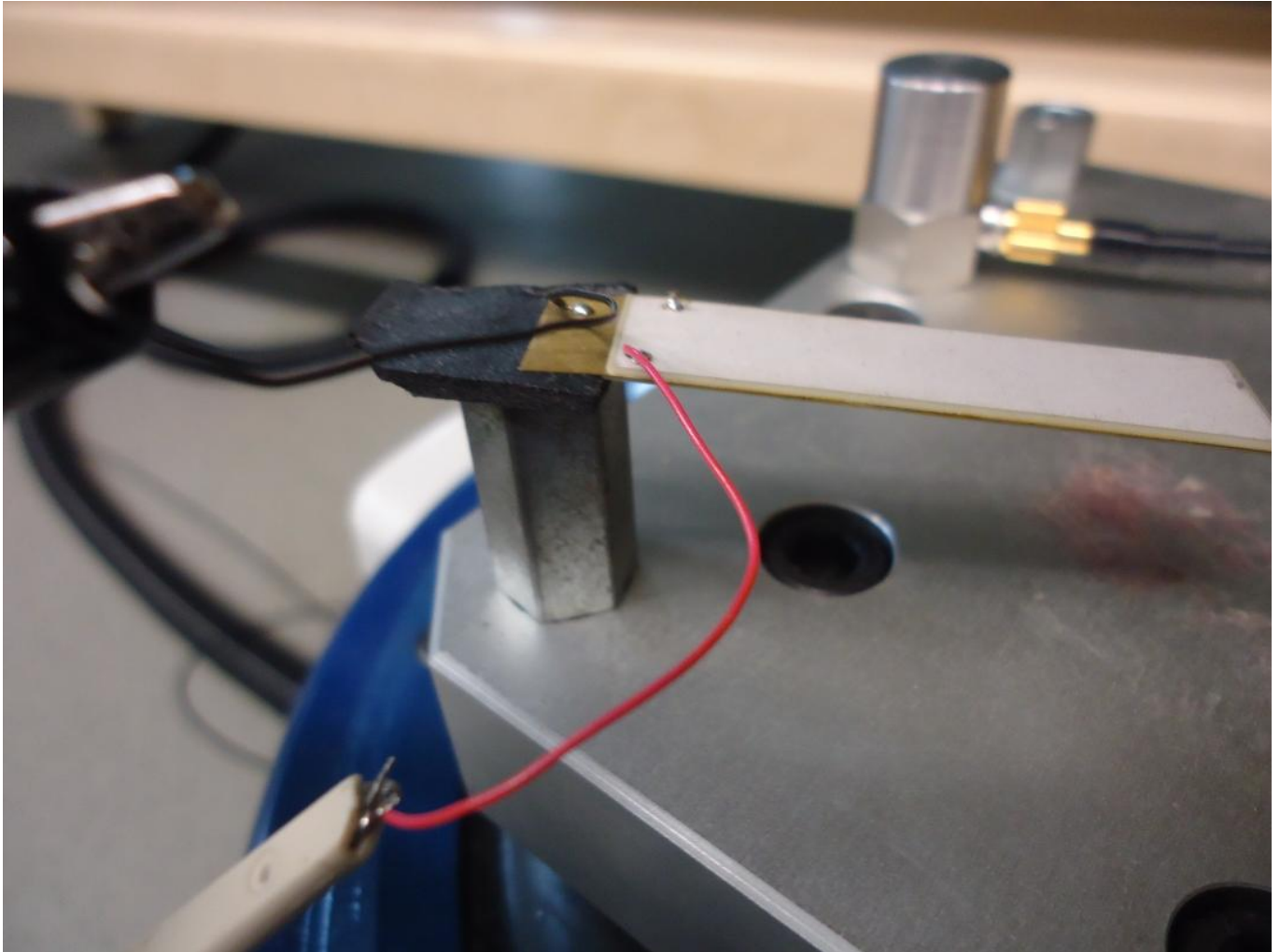
**APPENDIX E**  
**DYNAMIC VIBRATION SHAKER (IMV) - UTP BLOCK 18**



**APPENDIX F**  
**DYNAMIC SIGNAL ANALYZER – UTP BLOCK 18**



**APPENDIX G**  
**THE DESIGNED HARVESTING CANTILEVER PLACED ON**  
**THE SHAKER FOR EXPERIMENTAL ANALYSIS**



**APPENDIX H**  
**COMPLETE EXPERIMENTAL ANALYSIS – UTP BLOCK 18**

